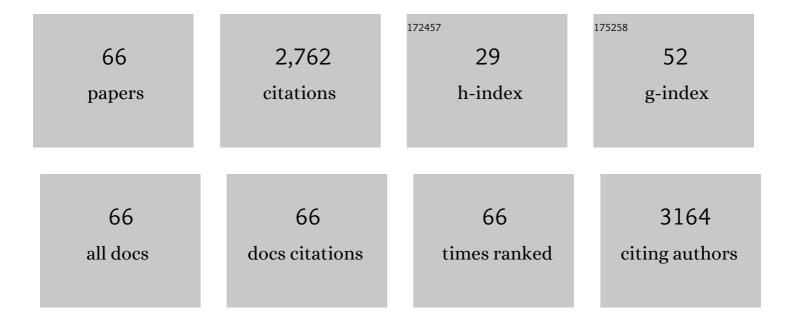
M MartÃ-nez-Escandell

List of Publications by Year in descending order

Source: https://exaly.com/author-pdf/6699901/publications.pdf

Version: 2024-02-01



#	Article	IF	CITATIONS
1	High‧urfaceâ€Area Carbon Molecular Sieves for Selective CO ₂ Adsorption. ChemSusChem, 2010, 3, 974-981.	6.8	316
2	Effect of the porous structure in carbon materials for CO2 capture at atmospheric and high-pressure. Carbon, 2014, 67, 230-235.	10.3	187
3	Methane hydrate formation in confined nanospace can surpass nature. Nature Communications, 2015, 6, 6432.	12.8	187
4	High-Pressure Methane Storage in Porous Materials: Are Carbon Materials in the Pole Position?. Chemistry of Materials, 2015, 27, 959-964.	6.7	178
5	Ultrahigh CO2 adsorption capacity on carbon molecular sieves at room temperature. Chemical Communications, 2011, 47, 6840.	4.1	166
6	An activated carbon monolith as an electrode material for supercapacitors. Carbon, 2009, 47, 195-200.	10.3	158
7	Semicokes from pitch pyrolysis: mechanisms and kinetics. Carbon, 1999, 37, 363-390.	10.3	114
8	Paving the way for methane hydrate formation on metal–organic frameworks (MOFs). Chemical Science, 2016, 7, 3658-3666.	7.4	103
9	Carbon foam prepared by pyrolysis of olive stones under steam. Carbon, 2006, 44, 1448-1454.	10.3	82
10	Pyrolysis of petroleum residues. Carbon, 2000, 38, 535-546.	10.3	76
11	Micro/Mesoporous Activated Carbons Derived from Polyaniline: Promising Candidates for CO ₂ Adsorption. Industrial & Engineering Chemistry Research, 2014, 53, 15398-15405.	3.7	66
12	The combined effect of porosity and reactivity of the carbon preforms on the properties of SiC produced by reactive infiltration with liquid Si. Carbon, 2009, 47, 2200-2210.	10.3	58
13	Production of binderless activated carbon monoliths by KOH activation of carbon mesophase materials. Carbon, 2008, 46, 384-386.	10.3	55
14	A site energy distribution function from Toth isotherm for adsorption of gases on heterogeneous surfaces. Physical Chemistry Chemical Physics, 2011, 13, 5753.	2.8	55
15	High saturation capacity of activated carbons prepared from mesophase pitch in the removal of volatile organic compounds. Carbon, 2010, 48, 548-556.	10.3	53
16	Very high methane uptake on activated carbons prepared from mesophase pitch: A compromise between microporosity and bulk density. Carbon, 2015, 93, 11-21.	10.3	52
17	Pyrolysis of petroleum residues: I. Yields and product analyses. Carbon, 1999, 37, 1567-1582.	10.3	46
18	Hydrogen adsorption on KOH activated carbons from mesophase pitch containing Si, B, Ti or Fe. Carbon, 2010, 48, 636-644.	10.3	41

M MartÃnez-Escandell

#	Article	IF	CITATIONS
19	Pyrolysis of petroleum residues: analysis of semicokes by X-ray diffraction. Carbon, 1999, 37, 1627-1632.	10.3	38
20	A continuous site energy distribution function from Redlich–Peterson isotherm for adsorption on heterogeneous surfaces. Chemical Physics Letters, 2010, 492, 187-192.	2.6	38
21	Methane hydrate formation in the confined nanospace of activated carbons in seawater environment. Microporous and Mesoporous Materials, 2018, 255, 220-225.	4.4	37
22	Influence of the oxygen-containing surface functional groups in the methane hydrate nucleation and growth in nanoporous carbon. Carbon, 2017, 123, 299-301.	10.3	34
23	CO2 activation of olive stones carbonized under pressure. Carbon, 2001, 39, 320-323.	10.3	33
24	The role of carbon biotemplate density in mechanical properties of biomorphic SiC. Journal of the European Ceramic Society, 2009, 29, 465-472.	5.7	33
25	Non-porous reference carbon for N2 (77.4 K) and Ar (87.3 K) adsorption. Carbon, 2014, 66, 699-704.	10.3	33
26	Manufacture of Biomorphic SiC Components with Homogeneous Properties from Sawdust by Reactive Infiltration with Liquid Silicon. Journal of the American Ceramic Society, 2010, 93, 1003-1009.	3.8	32
27	Selective Hydrogenation of Cinnamaldehyde over (111) Preferentially Oriented Pt Particles Supported on Expanded Graphite. Catalysis Letters, 2009, 133, 267-272.	2.6	30
28	Novel synthesis of a micro-mesoporous nitrogen-doped nanostructured carbon from polyaniline. Microporous and Mesoporous Materials, 2015, 218, 199-205.	4.4	30
29	Freezing/melting of water in the confined nanospace of carbon materials: Effect of an external stimulus. Carbon, 2020, 158, 346-355.	10.3	29
30	Influence of pressure variations on the formation and development of mesophase in a petroleum residue. Carbon, 1999, 37, 445-455.	10.3	26
31	Self-sintering of carbon mesophase powders: effect of extraction/washing with solvents. Carbon, 1999, 37, 1662-1665.	10.3	24
32	Preparation of mesophase pitch doped with TiO2 or TiC particles. Journal of Analytical and Applied Pyrolysis, 2007, 80, 477-484.	5.5	22
33	KOH activation of carbon materials obtained from the pyrolysis of ethylene tar at different temperatures. Fuel Processing Technology, 2013, 106, 402-407.	7.2	22
34	Effect of additives in the nucleation and growth of methane hydrates confined in a high-surface area activated carbon material. Chemical Engineering Journal, 2020, 388, 124224.	12.7	22
35	Heat of adsorption and binding affinity for hydrogen on pitch-based activated carbons. Chemical Engineering Journal, 2011, 168, 972-978.	12.7	21
36	Pyrolysis of petroleum residues. Carbon, 2001, 39, 61-71.	10.3	20

#	Article	IF	CITATIONS
37	Improved mechanical stability of HKUST-1 in confined nanospace. Chemical Communications, 2015, 51, 14191-14194.	4.1	19
38	Highâ€Performance of Gas Hydrates in Confined Nanospace for Reversible CH ₄ /CO ₂ Storage. Chemistry - A European Journal, 2016, 22, 10028-10035.	3.3	19
39	Well-defined meso/macroporous materials as a host structure for methane hydrate formation: Organic versus carbon xerogels. Chemical Engineering Journal, 2020, 402, 126276.	12.7	19
40	CO2 adsorption on crystalline graphitic nanostructures. Journal of CO2 Utilization, 2014, 5, 60-65.	6.8	17
41	Neural network and principal component analysis for modeling of hydrogen adsorption isotherms on KOH activated pitch-based carbons containing different heteroatoms. Chemical Engineering Journal, 2010, 159, 272-279.	12.7	16
42	A Continuous Binding Site Affinity Distribution Function from the Freundlich Isotherm for the Supercritical Adsorption of Hydrogen on Activated Carbon. Journal of Physical Chemistry C, 2010, 114, 13759-13765.	3.1	15
43	HKUST-1@ACM hybrids for adsorption applications: A systematic study of the synthesis conditions. Microporous and Mesoporous Materials, 2017, 237, 74-81.	4.4	15
44	Structural Flexibility in Activated Carbon Materials Prepared under Harsh Activation Conditions. Materials, 2019, 12, 1988.	2.9	15
45	Co-pyrolysis of an aromatic petroleum residue with triphenylsilane. Carbon, 2001, 39, 1001-1011.	10.3	12
46	Reverse Hierarchy of Alkane Adsorption in Metal–Organic Frameworks (MOFs) Revealed by Immersion Calorimetry. Journal of Physical Chemistry C, 2019, 123, 11699-11706.	3.1	12
47	Modification of the sintering behaviour of mesophase powder from a petroleum residue. Carbon, 2002, 40, 2843-2853.	10.3	10
48	Diffusionâ€Barrierâ€Free Porous Carbon Monoliths as a New Form of Activated Carbon. ChemSusChem, 2012, 5, 2271-2277.	6.8	8
49	Preparation of Porous Carbons from Petroleum Pitch and Polyaniline by Thermal Treatment for Methane Storage. Industrial & Engineering Chemistry Research, 2020, 59, 5775-5785.	3.7	8
50	Production of High-Strength Carbon Artifacts from Petroleum Residues:  Influence of the Solvent Used to Prepare Mesophase Powder. Energy & Fuels, 2002, 16, 1087-1094.	5.1	6
51	Adsorption on Heterogeneous Surfaces: Site Energy Distribution Functions from Fritz–Schlüender Isotherms. ChemPhysChem, 2010, 11, 2555-2560.	2.1	6
52	Production of nanoTiC–graphite composites using Ti-doped self-sintering carbon mesophase powder. Journal of the European Ceramic Society, 2013, 33, 583-591.	5.7	6
53	Manufacturing and high heat-flux testing of brazed actively cooled mock-ups with Ti-doped graphite and CFC as plasma-facing materials. Physica Scripta, 2009, T138, 014062.	2.5	5
54	Preparation of high metal content nanoporous carbon. Fuel Processing Technology, 2013, 115, 115-121.	7.2	5

#	Article	IF	CITATIONS
55	Chemistry of the co-pyrolysis of an aromatic petroleum residue with a pyridine–borane complex. Carbon, 2003, 41, 549-561.	10.3	4
56	Effect of boron carbide particle addition on the thermomechanical behavior of carbon matrix silicon carbide particle composites. Carbon, 2003, 41, 1096-1099.	10.3	4
57	Preparation of graphite/nano-SiC composites by co-pyrolysis of a petroleum residue with phenylsilanes. Journal of Analytical and Applied Pyrolysis, 2008, 83, 137-144.	5.5	4
58	Micromesoporous Activated Carbons as Catalysts for the Efficient Oxidation of Aqueous Sulfide. Langmuir, 2017, 33, 11857-11861.	3.5	4
59	Sinterability enhancement in semicokes obtained by controlled pyrolysis of a petroleum residue. Journal of Analytical and Applied Pyrolysis, 2008, 82, 163-169.	5.5	3
60	Activated carbon materials with a rich surface chemistry prepared from L-cysteine amino acid. Fluid Phase Equilibria, 2022, 558, 113446.	2.5	3
61	A new parameter relating the properties of semicokes and the resulting sintered carbons. Carbon, 1995, 33, 1182-1184.	10.3	2
62	Compilation of erosion yields of metal-doped carbon materials by deuterium impact from ion beam and low temperature plasma. Journal of Nuclear Materials, 2011, 417, 612-615.	2.7	2
63	The scientific impact of Francisco RodrÃguez-Reinoso in carbon research and beyond. Carbon, 2021, 179, 275-287.	10.3	2
64	Carbon-based monoliths with improved thermal and mechanical properties for methane storage. Fuel, 2022, 324, 124753.	6.4	2
65	Porosity determination in doped graphites using small-angle neutron scattering measurements. Journal of Physics: Conference Series, 2012, 340, 012102.	0.4	1
66	CO2 Adsorption in Activated Carbon Materials. Engineering Materials, 2021, , 139-152.	0.6	1